



A multi-scale and multi-mechanism approach for the fracture toughness assessment of polymer nanocomposites



M. Quaresimin*, M. Salviato, M. Zappalorto

Department of Management and Engineering, University of Padova, Stradella San Nicola 3, 36100 Vicenza, Italy

ARTICLE INFO

Article history:

Received 8 August 2013

Received in revised form 13 November 2013

Accepted 15 November 2013

Available online 28 November 2013

Keywords:

- A. Nanoparticles
- B. Fracture toughness
- B. Interphase

ABSTRACT

In the present work, a multi-scale modelling strategy to assess the fracture toughness of nanoparticle filled thermosetting polymers is presented. The model accounts for the main damaging mechanisms arising in this kind of materials, i.e. nanoparticle debonding, plastic yielding of nanovoids and plastic shear banding of the polymer. Further, the proposed analytical framework considers the influence of an interphase around nanoparticles, a particular feature of nanocomposites.

Comparison of the theory to a bulk of experimental data from the literature shows a very good agreement.

© 2013 Elsevier Ltd. All rights reserved.

1. Introduction

Nanotechnology has recently emerged as a suitable tool to optimise properties of materials by designing their internal structure at the very nanoscale thus assisting in the achievement of desirable combinations of physical and mechanical properties [1–3]. However, to fully exploit the potential benefits of nanomodification, appropriate models able to soundly predict the macroscale mechanical properties from material structure need to be developed.

With the aim to explain the significant improvements of polymer toughness achievable with low nanofiller contents and considering the importance of the several damaging mechanisms that might take place at the nanoscale, some authors have recently suggested to use a “multi-mechanism” modelling strategy [4–8].

However, modelling the effects of nanoscale damaging mechanisms on macroscale properties is far from easy, essentially because at that length scale classical micromechanics is no longer valid. Instead, the adoption of a multi-scale strategy is necessary in order to describe the nanocomposite material behaviour, physically and mathematically, in each individual scale of interest.

In the recent literature several authors dealt with the analysis of toughening mechanisms in nanocomposites.

Chen et al. [9] carried out a theoretical study on the amount of energy dissipated by interfacial debonding of nanoparticles and provided a close form solution for the critical detachment stress. The size distribution of particles and the debonding probability

were included into the analytical formulation using a logarithmic normal distribution and the Weibull distribution function, respectively.

Some years later, the present authors refined the analysis carried out in [9] studying the effects of a small interphase zone embedding the nanoparticle [10] and of surface elastic constants [11] on the critical debonding stress. In both cases, the range of the nanoparticle radii where those effects are significant was proved to be limited to the nanoscale [10,11].

The energy dissipation phenomena due to particle debonding, voiding and subsequent yielding of the polymer have been analysed by Lauke [4] who used a simple geometrical model of particle–particle interaction in a regular particle arrangement. By further applying a critical stress criterion, Lauke found a dissipation zone which was independent of the particle diameter and justified the increase of crack resistance with decreasing particle size by the increase in the specific debonding energy [4].

Williams [5] re-analysed in detail the toughening of particle filled polymers assuming that plastic void growth around debonded or cavitated particles is the dominant mechanism for energy dissipation. He assumed a tri-axial state of stress around the spherical particle and supposed the debonding and cavitation conditions to be controlled by either surface energy or the cohesive energy of the particle. Williams further noted that, even if the debonding process is generally considered to absorb little energy, it is essential to reduce the constraint at the crack tip and, in turn, to allow the epoxy polymer to deform plastically via a void-growth mechanism. A similar result was found also by the present authors [12].

Hsieh et al. [6,7] studied the fracture toughness improvements resulting from nanomodification of epoxy resins with silica nanoparticles. Based on experimental observations, they identified

* Corresponding author. Tel.: +39 0444 998723; fax: +39 0444 998888.
E-mail address: marino.quaresimin@unipd.it (M. Quaresimin).

two dominant mechanisms responsible of toughening improvements, namely localised shear banding of the polymer and particle debonding followed by subsequent plastic void growth. They finally adapted a previous model due to Huang and Kinloch [13] for rubber modified epoxy polymers to predict the fracture toughness improvements resulting from nanomodification.

The investigations in [4–7] support the idea, recently formulated also by the present authors [8], that the most effective approach to predict the nanocomposite toughness is a “multi-mechanism” modelling strategy, in which the contribution of each mechanism is appropriately determined and weighted according to the specific case (accounting for the type, the morphology and the functionalisation of the nanofiller). Accordingly the nanocomposite fracture toughness can be written as the summation of the fracture toughness of the unloaded matrix, G_{im} , and the fracture toughness improvement due to the each i -th damaging mechanism, ΔG_i .

Great efforts have been recently devoted by the present authors to develop analytical formulations for ΔG_i contributions due to the most relevant toughening mechanisms occurring in nanoparticle filled polymer resins. Among these, debonding of nanoparticles followed by plastic yielding of nanovoids [12] and plastic shear banding of the polymer [14] have been analysed. The major novelty of these recent works, with respect to those in the previous literature dealing with the same subject [4–7], lays on the fact that the effect of an interphase zone surrounding the nanoparticle, characterised by mechanical properties different from those of the constituents, is explicitly considered.

Starting from the analytical models developed in previous works [12,14], the main aim of the present paper is to provide a multiscale analytical procedure useful to evaluate the overall fracture toughness of a polymer/nanoparticle nanocomposite.

The proposed multiscale-multimechanism model accounts for particle debonding, plastic yielding of nanovoids and shear banding of the polymer, thus allowing to quantify the effect of the associated energy dissipation phenomena on the overall fracture toughness of the material. Theoretical predictions for the nanocomposite fracture toughness are compared with a large bulk of experimental data taken from the literature, showing a satisfactory agreement.

2. Description of the multiscale strategy adopted for the analysis

Nanocomposites are endowed with a hierarchical structure, which encompasses the nano and the macro length-scales. A successful prediction of the mechanical properties of these materials thus requires models able to account for the phenomena peculiar of each length-scale and to bridge their effects from the nano scale to the macroscale.

According to [8] it can be stated that, generally speaking, three stages should be addressed in nanocomposite modelling, each stage being referred to a specific length scale and to be tackled with the aid of dedicated models. Basic models can be finally assembled to build a multiscale modelling strategy.

The present authors have recently proposed a hierarchical multiscale strategy according to which the nanocomposite material is mathematically decomposed into three systems of interest.

Briefly:

- the macroscale system is thought of as an amount of material over which all the mechanical quantities (such as stresses and strains) are regarded as averaged values [15] and are supposed to be representative of the overall material behaviour;
- the micro-scale system is thought of as being sufficiently small to be regarded, mathematically, as an infinitesimal volume of

the macro-scale one. At the same time it has to be, by definition, large enough to be statistically representative of the properties of the material system (described by a *Representative Volume Element*, RVE);

- the nanoscale system represents a single unit cell of those compounding the micro-scale system and it accounts for the material morphology at the nanoscale.
- The link between different system is obtained through the combined use of the Mori–Tanaka theorem and the Global Concentration Tensors of Eshelby dilute solution (see Fig. 1). Accordingly, the stress acting on the boundary of a single nano-inhomogeneity (nanoscale) is approximated as:

$$\sigma_n = \mathbf{H} : \left\{ \frac{1}{V} \int_V \hat{\sigma} dV \right\} = \mathbf{H} : \sigma \quad (1)$$

where \mathbf{H} is the Global Concentration Tensors of Eshelby dilute solution [10], and $\frac{1}{V} \int_V \hat{\sigma} dV$ is the mean value for the stress fields over the RVE which, thanks to Mori–Tanaka theorem equates the macro-scale stress field.

The system under investigation at the nanoscale, shown in Fig. 2a, is constituted by:

- a spherical nanoparticle (nanovoid) of radius r_0 ;
- a shell-shaped interphase of external radius a and thickness t ($a = t + r_0$) and uniform properties;
- a volume of matrix of which the size are much greater than a and r_0 .

This system accounts for molecular interactions at the nanoscale through the size and elastic properties of the interphase layer [10]. Unfortunately there is a lack of reliable data about the law of variation of the interphase properties across its thickness [16]. This urged some authors [10,12,14,16–19] to assume that a through-the-thickness average is representative of the overall property distribution within the interphase. Consequently, the interphase is supposed to be homogeneous and isotropic.

The system at the macro-scale is constituted, instead, of a cracked nano-modified matrix (see again Fig. 2b) under mode I loadings. It is assumed that the macroscopic stress fields due to the crack, given by Irwin’s solution (see [14] for more details) enhances the formation of a process zone containing all the nanoparticles subjected to damage, thus promoting energy dissipation at the nanoscale, and resulting, in turn, in an overall fracture toughness improvements of the nanocomposite.

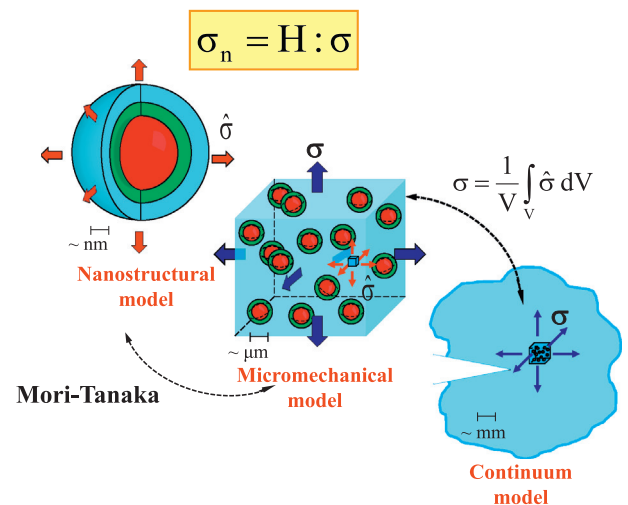


Fig. 1. Multiscale strategy and systems of interest.

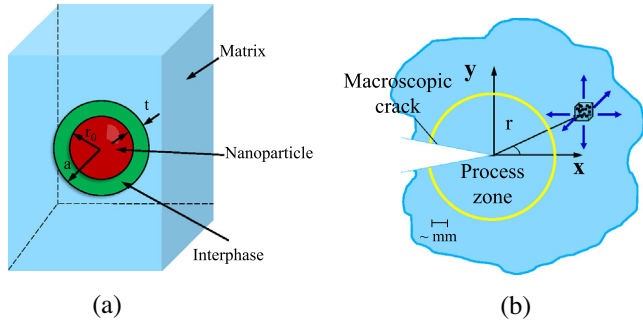


Fig. 2. Description of the systems under analysis at the nanoscale (a) and at the macroscale (b).

As discussed in the introduction, on the basis of recent experimental observations [6,7], it can be reasonably assumed that several nanoscale damaging mechanisms might simultaneously contribute to the overall fracture toughness of the nanocomposite. Accordingly, the nanocomposite toughness can be written as

$$G_{Ic} = G_{Im} + \sum_i \Delta G_i \quad (2)$$

where G_{Im} is the toughness of the unloaded matrix and ΔG_i is the toughness improvement due to the i -th damaging mechanism. Denoting with U_i the energy produced at the nanoscale by a particular mechanism, the corresponding microscale strain energy density is:

$$u_i = U_i \times \frac{3f_{p0}}{4\pi r_0^3} \quad (3)$$

where f_{p0} is the volume fraction of nanoparticles. Finally, the fracture toughness enhancement due to the single damage mechanism, to be inserted in Eq. (2), can be determined as [12,14,20]:

$$\Delta G_i = 2 \times \int_0^{\rho_i} u_i \, d\rho \quad (4)$$

where ρ_i denotes the extension of the damaged zone ahead of the crack tip.

3. Modelling of the fracture toughness enhancements due to the different damaging mechanisms

It is acknowledged in the literature that the two dominant mechanisms responsible of toughening improvements for polymers reinforced by rigid nanoparticles (such as silica or alumina nanoparticles) are the localised shear banding of the polymer and particle debonding followed by subsequent plastic yielding of nanovoids [6,7,12,14].

In the following sections close form expressions useful to evaluate the fracture toughness improvements, ΔG_i , due to the above mentioned mechanisms are given. Finally, in Section 3.4 a unified expression for the overall nanocomposite fracture toughness is derived.

3.1. Fracture toughness enhancement due to particle debonding

In Ref. [12] it is assumed that in a damaged region close to the crack tip (Debonding Region, DBR) the high level of the crack-induced hydrostatic stress promotes debonding of nanoparticles. The microscale strain energy density dissipated by this mechanism can be calculated as:

$$u_{db} = 3 \frac{\gamma_{db}}{r_0} f_{p0} \quad (5)$$

where f_{p0} is the nanofiller volume fraction and γ_{db} is the interfacial fracture energy. The macroscale increment in terms of Strain Energy Release Rate due to this mechanism can be estimated inserting Eq. (5) into (4):

$$\Delta G_{db} = f_{p0} \times \psi_{db} \times G_{Ic} \quad (6)$$

where G_{Ic} is the fracture toughness of the nanocomposite and ψ_{db} is a term accounting for energy dissipation [12]

$$\psi_{db} = \frac{2}{3\pi} \times \frac{\gamma_{db}}{r_0} \times \frac{1 + \nu_o}{1 - \nu_o} \times \frac{E_o}{\sigma_{cr}^2 (C_h)^2} \quad (7)$$

In Eq. (7) E_o and ν_o are the elastic properties of the nanocomposite, σ_{cr} is the critical debonding stress [10]:

$$\sigma_{cr} \cong \sqrt{\frac{4\gamma_{db}}{r_0} \frac{E_m}{1 + \nu_m} \sqrt{\frac{\chi(4 + \xi) - \xi(\chi - 1)(r_0/a)^3}{4 + \xi + 4(\chi - 1)(r_0/a)^3}}} \quad (8a)$$

and C_h is the reciprocal of the hydrostatic part of the global stress concentration tensor [9]

$$C_h = \frac{K_m (\xi + 4)(3K_p/G_m + 4\chi)}{K_p (\xi + 4\chi)(3K_m/G_m + 4)} + \frac{(4\xi - 12K_p/G_m)(1 - \chi)}{(\xi + 4\chi)(3K_m/G_m + 4)} \left(\frac{r_0}{a}\right)^3 \quad (8b)$$

where E_m and ν_m are the elastic modulus and Poisson's ratio of the matrix, K_m , K_a and K_p the bulk moduli of the matrix, the interphase and the nanoparticle, G_m and G_a are the shear elastic moduli of the matrix and the interphase, $\chi = G_a/G_m$ and $\xi = 3K_a/G_m$

3.2. Fracture toughness enhancement due to the plastic yielding of nanovoids

Debonding of nanoparticles creates a number of nanovoids of the same diameter of the initial nanoparticles. Whenever the stress field around a nanovoid is high enough it might cause local yielding of the nanovoids. Through a multiscale analysis of the energy dissipation process due to plastic yielding of nanovoids, Zappalorto et al. [12] provided the following expression for the fracture toughness enhancement due to this mechanism:

$$\Delta G_{py} = f_{p0} \times \psi_p \times G_{Ic} \quad (9)$$

where G_{Ic} is the fracture toughness of the nanocomposite and ψ_p is a term accounting for energy dissipation and can be written as:

$$\psi_p = \frac{4}{9\pi C_h} \cdot \frac{E_o}{E_m} \cdot \frac{(1 + \nu_o)(1 + \nu_m)}{1 - \nu_o} \times \frac{\sigma_{Ym}}{\sigma_{cr}} \left(\frac{a}{r_0}\right)^3 \times \left(1 - \frac{\sigma_{Ya}}{\sigma_{Ym}}\right) e^{\left(3C_h \frac{\sigma_{cr}}{\sigma_{Ym}} - 1\right)} \quad (10a)$$

for an elastic perfectly plastic behaviour of the matrix and the interphase or as:

$$\psi_p = \left\{ \frac{2}{9\pi C_h} \cdot \frac{1 + \nu_o}{1 - \nu_o} \cdot \frac{E_o}{G_m} \cdot \frac{\sigma_{Ym}}{\sigma_{cr}} \cdot \left(\frac{a}{r_0}\right)^3 \cdot \left[\frac{3C_h \frac{\sigma_{cr}}{\sigma_{Ym}} - (1 - n_m)}{n_a \frac{\sigma_{Ya}}{\sigma_{Ym}} \left(\frac{\sigma_{Ym}}{\sigma_{Ya}}\right)^{\frac{1}{n_a}} \left[\left(\frac{a}{r_0}\right)^{3/n_a} - 1\right] + n_m} \right]^{n_m} \right\} \quad (10b)$$

for a hardening behaviour of the matrix and the interphase, where σ_{Ym} and σ_{Ya} are the yield stress of the matrix and the interphase, n_m and n_a are the hardening exponents of the matrix and the interphase, respectively.

Table 1

Summary of all the systems considered, related references and the properties used in the present analysis.

Series	Reference	Matrix	Nanofiller	r_0 (nm)	t (nm)	E_m (MPa)	χ	σ_{ym} (MPa)	σ_{ycm} (MPa)	γ_{fm}
1	Hsieh et al. [7]	DGEBA	SiO ₂ nanoparticles (Nanopox F400)	10	4	2960	1.7	88	120	0.75
2	Zamanian et al. [23]	DGEBA	Nonporous silica (Aerosil 200)	6	4	3530	1.7	88.15	96.12	0.72
3	Zamanian et al. [23]	DGEBA	Nonporous silica (Aerosil 90)	10	4	3530	1.7	88.15	96.12	0.72
4	Zamanian et al. [23]	DGEBA	Nonporous silica (OX50)	20	4	3530	1.7	88.15	96.12	0.72
5	Dittanet and Pearson [24]	DER331	SiO ₂ nanoparticles (nano-SiO ₂)	11.5	4	3500	1.7	85	107.2	0.71
6	Dittanet and Pearson [24]	DER331	SiO ₂ nanoparticles (nano-SiO ₂)	37	4	3500	1.7	85	107.2	0.71
7	Dittanet and Pearson [24]	DER331	SiO ₂ nanoparticles (nano-SiO ₂)	85	4	3500	1.7	85	107.2	0.71
8	Ma et al. [25]	DGEBA, Araldite-F	SiO ₂ nanoparticles (Nanopox F400)	10	4	3200	1.7	88.2	120 ^a	0.4 ^a
9	Ma et al. [25]	DGEBA	SiO ₂ nanoparticles (Nanopox F400)	10	4	2750	1.7	57.1	120 ^a	0.72 ^a
10	Chen et al. [26]	DGEBA	SiO ₂ nanoparticles (MEK-ST)	6	4	2760	1.7	86	120 ^a	0.75 ^a
11	Liang et al. [27]	DGEBA/F	SiO ₂ nanoparticles (Nanopox E430)	10	4	2410	1.7	50 ^a	94.4	0.71
12	Liang et al. [27]	DGEBA	SiO ₂ nanoparticles (3 M)	40	4	2410	1.7	50 ^a	94.4	0.71

^a These data were not provided by the Authors of the original works. These properties have been supposed by the present authors on the basis of similar systems.

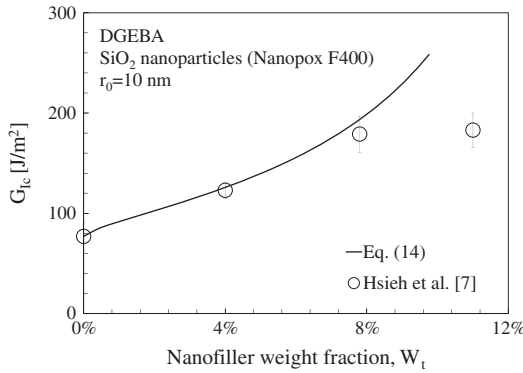


Fig. 3. Comparison between Eq. (14) (solid line) and the experimental data from DGEBA/Nanopox system [7].

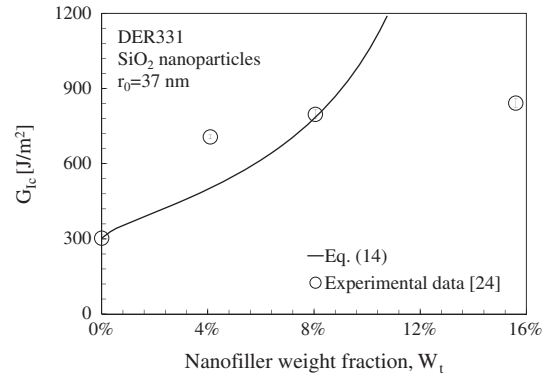


Fig. 5. Comparison between Eq. (14) (solid line) and the experimental data from DER331/SiO₂ nanoparticles [24].

3.3. Fracture toughness enhancement due to localised shear banding

In a damaged region close to the crack tip (Shear Banding Region, SBR) the stress concentrations around nanoparticles might promote local shear yielding, with the formation of less or more pronounced plastic shear bands [14]. Through a multiscale analysis of the process the following expression for the fracture toughness enhancement linked to this mechanism was provided [14]:

$$\Delta G_{SB} = f_{p0} \times \psi_{SB} \times G_{1c} \tag{11}$$

where ψ_{SB} accounts for the energy dissipation at the nanoscale:

$$\psi_{SB} = \frac{I_{SB}}{4\pi\sigma_{yca}^2(1 - \mu/\sqrt{3})^2} \frac{E_o}{1 - \nu_o^2} \times \Gamma \tag{12}$$

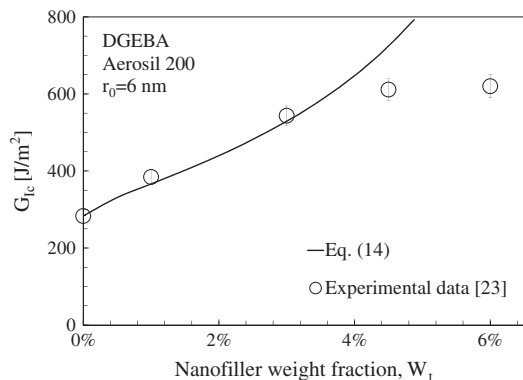


Fig. 4. Comparison between Eq. (14) (solid line) and the experimental data from DGEBA/Aerosil 200 system [23].

In Eq. (12), μ is a dimensionless pressure coefficient, σ_{yca} is the interphase yielding stress under compression, whereas function Γ quantifies the energy produced at the nanoscale and I_{SB} accounts for the stress concentration around nanoparticles [14]:

$$\Gamma = \tau_{ym}\gamma_{fm} \left\{ \left(\frac{\pi}{6f_{p0}} \right)^{\frac{1}{2}} - \frac{52}{63} \frac{\tau_{ya}\gamma_{fa}}{\tau_{ym}\gamma_{fm}} - \left(1 - \frac{\tau_{ya}\gamma_{fa}}{\tau_{ym}\gamma_{fm}} \right) \frac{[32Q(\frac{1}{3} + \frac{\bar{a}^4}{5}) + \frac{\bar{a}^2}{315}(45 - 32\bar{a}^4Z + 128\bar{a}^6M)]}{21} \right\} \tag{13a}$$

$$I_{SB} = \frac{1}{2\pi} (pH_{vM}^2 + k\mu H_h H_{vM} + j\mu^2 H_h^2) \tag{13b}$$

$$\begin{aligned} \bar{a} &= \frac{a}{r_0} & Q &= \sqrt{\bar{a}^2 - 1} & M &= \bar{a} - Q \\ S &= 105\bar{a} - 88Q & Z &= 9\bar{a} - 7Q \end{aligned} \tag{13c}$$

In Eq. (13a) τ_{ym} and τ_{ya} are the shear yielding stress of the matrix and of the interphase, whereas γ_{fm} and γ_{fa} are the shear fracture strains.

In Eq. (13b), parameters p, k, j are functions of the Poisson's ratio, $H_h = 1/C_h$ and H_{vM} is the deviatoric component of the global stress concentration tensor. It can be evaluated numerically or analytically [14,17].

3.4. Overall fracture toughness of the nanocomposites

As far as the fracture toughness improvements due to each relevant damaging mechanism, ΔG_i , are known, the overall nanocomposite fracture toughness can be estimated according to Eq. (2).

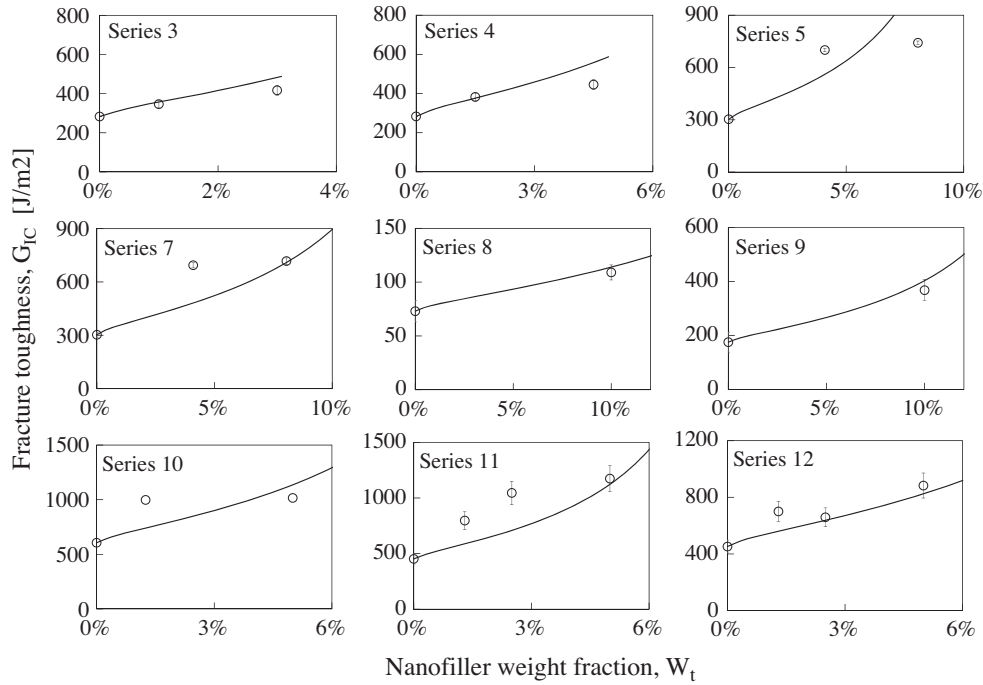


Fig. 6. Summary of the comparisons between Eq. (14) (solid line) and the experimental data from Series 3–5, and 7–12 (see Table 1).

Thus, substituting Eqs. (6), (9), and (11) into (2) one obtains the overall fracture toughness of the nanocomposite as a function of G_{Im} and f_{p0}

$$G_{IC} = \frac{G_{Im}}{1 - f_{p0}(\psi_{db} + \psi_p + \psi_{SB})} \quad (14)$$

4. Estimation of interphase size and elastic properties

In order to apply Eq. (14) the properties and size of the interphase need to be determined.

The elastic properties and the thickness of the interphase can be computed by means of numerical simulations carried out within the frame of MD as done for example by Odegard et al. [18] and Yu et al. [19], which provide, as outputs, the radial extension of the interphase as well as the elastic properties averaged through the thickness.

Alternatively, for a specific system, they could be determined *a posteriori* by fitting the experimental values for the elastic properties of the nanocomposite by a multi-phase, micromechanical model.

In this paper we have used the model provided by Dunn and Ledbetter [21], who suggested:

$$K_0 = K_m + \frac{1}{3} \frac{f_{p0}(a/r_0)^3 (K_a - K_m) T_{pa}^H + f_{p0}(K_p - K_a) T_p^H}{1 - f_{p0} + f_{p0}(a/r_0)^3 T_{pa}^H} \quad (15)$$

where:

$$T_{pa}^H = 1 - 3\gamma_{0a} \left\{ \left(\frac{r_0}{a} \right)^3 \frac{K_p - K_m}{3\gamma_{0a}(K_p - K_m) + K_m} + \left[1 - \left(\frac{r_0}{a} \right)^3 \right] \frac{K_a - K_m}{3\gamma_{0a}(K_a - K_m) + K_m} \right\}$$

$$T_p^H = 1 - \frac{3\gamma_{0m}(K_p - K_m)}{3\gamma_{0m}(K_p - K_m) + K_m}$$

$$3\gamma_{0a} = (1 + \nu_a)/[3(1 - \nu_a)] \quad 3\gamma_{0m} = (1 + \nu_m)/[3(1 - \nu_m)] \quad (16)$$

The best fitting of elastic properties of nanocomposite materials using Eq. (15) allows to estimate the “optimum” combination of interphase elastic properties and size to be used in the proposed modelling strategy.

As highlighted by Eq. (10) and (13), in principle, the estimated value of the overall fracture toughness of the nanocomposite depends also on the strength and yield properties of the interphase. However, precise information on these interphase properties are unavailable. Accordingly, for the sake of simplicity, in this work we propose to equate all the yield and strength properties of the interphase to those of the matrix.

5. Model validation by comparison with experimental data

In this section, the theoretical estimations of the nanocomposite fracture toughness obtained by Eq. (14) are compared to a bulk of experimental data taken from the literature. A summary of the data used, the relevant references and the properties used in the analysis are reported in Table 1.

It is worth mentioning here that in some cases the authors explicitly provided, in the original work, all the data necessary to the analysis, while in other cases some data have been assumed by analogy with similar systems.

Initially the attention has been focused on the data by Hsieh et al. [7], on which an accurate reverse engineering analysis has been carried out in order to determine the elastic properties and the size of the interphase, using Eq. (15). The resulting best fitting values have been found to be $\chi = 1.7$ and $t = 4$ nm, respectively. As a second step, it has been verified that these values allow a satisfactorily accurate fitting of the elastic properties for all the other considered data so that the same values ($t = 4$ nm and $\chi = 1.7$) have been used for all the systems analysed in the present work.

It is interesting to note that $\chi = 1.7$ is very close to the value measured by Watcharotone et al. [22] for polymethyl-methacrylate via nanoindentation experiments on thin films coupled with finite element modelling.

For the sake of simplicity, the plastic properties of the interphase zone have been supposed to equate those of the matrix.

With reference to the data provided by Hsieh et al. [7], Fig. 3 shows a comparison between the fracture toughness predicted by Eq. (14) and experimental results. It is evident that for low filler

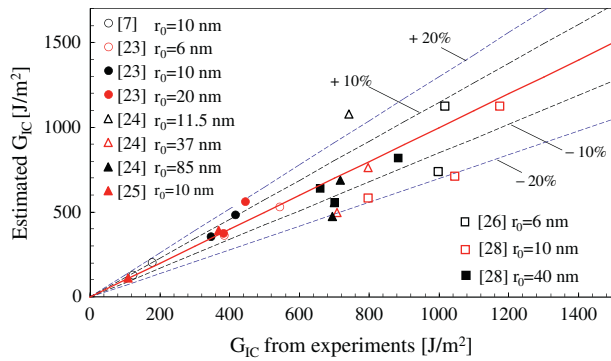


Fig. 7. Comparison between experimental values and the predicted values (Eq. (14)) of the fracture toughness for all the nanocomposite systems re-analysed in the present work.

weight fractions (up to 8%) the agreement is very satisfactory. Instead, for higher filler content, Eq. (14) predicts a monotonically increasing fracture toughness, while experimental results exhibit a plateau, commonly acknowledged as due to filler aggregation. This deviating behaviour of theoretical predictions with respect to experiments should not surprise the readers; indeed, as basic assumption of the proposed model, the nanofiller is supposed to be uniformly dispersed and distributed, neglecting the high tendency to agglomerate exhibited by nanoparticles beyond a certain value of the weight fraction. It is clear that this approximation hampers the application of the model to high nanofiller contents. On the other hand, the great potential of nanomodification lays on the achievement of significant improvements of polymer toughness at low nanofiller contents, while the knowledge of the material behaviour besides this zone of steep property increase is less important. Nevertheless an agglomeration model is going to be developed by the present authors.

A satisfactory agreement at low filler weight fraction is evident also in Fig. 4, where a comparison between the fracture toughness predicted through Eq. (14) and the experimental results provided by Zamanian et al. [23] is presented.

However, in few cases of those analysed, the agreement is less satisfactory. Fig. 5 for example, shows the data by Dittanet and Pearson [24]. In this case experimental data exhibit an initial very steep increase and then tend toward an almost constant value; the theoretical curve is not able to seize this trend, and an accurate prediction is possible only for the data at 8% Wt.

A summary of all the other data not discussed before is reported in Fig. 6: on the basis of the overall good agreement with the experimental data, it can be concluded that Eq. (14) allows, in general, a satisfactory estimation of the fracture toughness of polymers reinforced with nanoparticles.

Eventually, predicted values are plotted versus experimental values for all the analysed data in Fig. 7, limiting the attention only to low filler contents. The satisfactory agreement is confirmed: the majority of data fall within a $\pm 10\%$ scatter band, while a $\pm 20\%$ scatter band includes all the experimental set of data but one.

6. Conclusions

In the present work, a multi-scale multi-mechanism modelling strategy has been provided for the prediction of toughness increments caused by the emergence of debonding, plastic yielding and localised plastic shear bands in nanoparticle filled resins. The model is based on the quantification of the energy absorbed at the

lower scale and accounts for the emergence of an interphase, created by the inter- and supra-molecular interactions arising at the nano-scale, with mechanical properties different from those of the matrix. The model has been compared to a large bulk of experimental data collected from the literature, showing good agreements.

Acknowledgements

The financial support to the activity by Veneto Nanotech, the Italian cluster of Nanotechnology, is greatly acknowledged.

References

- [1] Ajayan PM, Schadler LS, Braun PV. Nanocomposite science and technology. Wiley-VCH; 2003, ISBN 3527303596.
- [2] Thostenson ET, Li C, Chou TW. Nanocomposites in context. *Compos Sci Technol* 2005;65:491–516.
- [3] Sumfleth J, Prehn K, Wichmann MHG, Wedekind S, Schulte K. A comparative study of the electrical and mechanical properties of epoxy nanocomposites reinforced by CVD- and arc-grown multi-wall carbon nanotubes. *Compos Sci Technol* 2010;70:173–80.
- [4] Lauke B. On the effect of particle size on fracture toughness of polymer composites. *Compos Sci Technol* 2008;68:3365–72.
- [5] Williams JG. Particle toughening of polymers by plastic void growth. *Compos Sci Technol* 2010;70:885–91.
- [6] Hsieh TH, Kinloch AJ, Masania K, Taylor AC, Sprenger S. The mechanisms and mechanics of the toughening of epoxy polymers modified with silica nanoparticles. *Polymer* 2010;51:6284–94.
- [7] Hsieh TH, Kinloch AJ, Masania K, Sohn Lee J, Taylor AC, Sprenger S. The toughness of epoxy polymers and fibre composites modified with rubber microparticles and silica nanoparticles. *J Mater Sci* 2010;45:1193–210.
- [8] Quaresimin M, Salviato M, Zappalorto M. Strategies for the assessment of nanocomposite mechanical properties. *Compos part B-Eng* 2012;43:2290–7.
- [9] Chen JK, Huang ZP, Zhu J. Size effect of particles on the damage dissipation in nanocomposites. *Compos Sci Technol* 2007;14:2990–6.
- [10] Zappalorto M, Salviato M, Quaresimin M. Influence of the interphase zone on the nanoparticle debonding stress. *Compos Sci Technol* 2011;72:49–55.
- [11] Salviato M, Zappalorto M, Quaresimin M. The effect of surface stresses on the critical debonding stress around nanoparticles. *Int J Fract* 2011;172:97–103.
- [12] Zappalorto M, Salviato M, Quaresimin M. A multiscale model to describe nanocomposite fracture toughness enhancement by the plastic yielding of nanovoids. *Compos Sci Technol* 2012;72:1683–91.
- [13] Huang Y, Kinloch AJ. Modelling of the toughening mechanisms in rubber-modified epoxy polymers. Part II A quantitative description of the microstructure-fracture property relationships. *J Mater Sci* 1992;27:2763–9.
- [14] Salviato M, Zappalorto M, Quaresimin M. Plastic shear bands and fracture toughness improvements of nanoparticle filled polymers: a multiscale analytical model. *Compos Part A-Appl S* 2013;48:144–52.
- [15] Timoshenko SP, Goodier JN. Theory of elasticity. 3rd ed. New York: McGraw-Hill; 1970.
- [16] Sevostianov I, Kachanov M. Effect of interphase layers on the overall elastic and conductive properties of matrix composites. Applications to nanosize inclusion. *Int J Solids Struct* 2007;44:1304–15.
- [17] Zappalorto M, Salviato M, Quaresimin M. Stress distributions around rigid nanoparticles. *Int J Fract* 2012;176:105–12.
- [18] Odegard GM, Clancy TC, Gates TS. Modeling of mechanical properties of nanoparticle/polymer composites. *Polymer* 2005;46:553–62.
- [19] Yu S, Yang S, Cho M. Multi-scale modeling of cross-linked epoxy nanocomposites. *Polymer* 2009;50:945–52.
- [20] Freund LB, Hutchinson JW. High-strain-rate crack growth in rate dependent plastic solids. *J Mech Phys Solids* 1985;33:169–91.
- [21] Dunn M, Ledbetter H. Elastic constants of composites reinforced by multiphase particles. *J Appl Mech* 1995;62:1023–8.
- [22] Watcharotone S, Wood CD, Friedrich R, Chen X, Qiao R, Putz K, et al. Interfacial and substrate effects on local elastic properties of polymers using coupled experiments and modeling of nanoindentation. *Adv Eng Mater* 2011;13:400–4.
- [23] Zamanian M, Mortezaei M, Salehnia B, Jam JE. Fracture toughness of epoxy polymer modified with nanosilica particles: particle size effect. *Eng Fract Mech* 2013;97:193–206.
- [24] Dittanet P, Pearson RA. Effect of silica nanoparticle size on toughening mechanisms of filled epoxy. *Polymer* 2012;53:1890–905.
- [25] Ma J, Mo M-S, Du X-S, Rosso P, Friedrich K, Kuan H-C. Effect of inorganic nanoparticles on mechanical property, fracture toughness and toughening mechanism of two epoxy systems. *Polymer* 2008;49:3510–23.
- [26] Chen C, Justice RS, Schaefer DW, Baur JW. Highly dispersed nanosilica-epoxy resins with enhanced mechanical properties. *Polymer* 2008;49:3805–15.
- [27] Liang YL, Pearson RA. Toughening mechanisms in epoxy-silica nanocomposites (ESNs). *Polymer* 2009;50:4895–905.